DESIGN CONSIDERATIONS FOR A RE-ENTRY VEHICLE THERMAL PROTECTION SYSTEM

J.H. Bridges[1] and F.D. Richmond[2]

Chance Vought Corp., Dallas, Texas

ABSTRACT

The design parameters for a re-entry vehicle thermal protection system are examined. These parameters are considered in the development of a thermal protection system which utilizes an optimum combination of a heat shield, high temperature insulation, metallic vapor barrier and Thermosorb -- a Vought developed high water content expendable heat sink.

INTRODUCTION

It is common knowledge that vehicles returning to Earth from orbital or space missions experience elevated surface temperatures due to aerodynamic heating. Although ablative and/or radiative cooling methods are used to limit surface temperatures, weight optimization leads to the use of the higher temperatures in order to use less ablative and more radiative cooling. The result is that the lightest surface system tends to be the one that operates at the highest temperature.

These high surface temperatures create the need for a system to prevent excessive temperatures within the vehicle. Such a system is possible by using a combination of insulation and heat sink in the vehicle walls, and it is that type of system that is the subject of this paper. First, an insulation is

Presented at the ARS Lunar Missions Meeting, Cleveland, Ohio, July 17-19, 1962.

The design considerations and conclusions presented are derived from work conducted on U.S. Air Force Contract AF33(616)-7829, "Structural integration of thermosorb", interim report (December 1961).

[1]Lead Engineer, Technologies R & D, Astronautics Division.

[2]Associate Engineer, Power and Environment, Astronautics Division.

used as partial protection against the high outside temperature. Second, a heat sink capable of absorbing and disposing of heat at compartment temperatures is used.

Vought Astronautics developed a high water content semi-solid heat sink material now known as Thermosorb. This material, illustrated in Fig. 1, is a high water content semi-solid gel retained by an open cell sponge and sealed in a thermoplastic container. The sponge provides mechanical retention for the acceleration-resistant gel. The container prevents evaporation during storage or space operations and melts upon exposure to re-entry heating to activate the system. Thermosorb has been subjected to vibration, "g"-loading, temperature variations, etc., to demonstrate its ability to perform satisfactorily under the various conditions of space travel.

While Thermosorb was being developed, a contract was negotiated with ASD for a Thermosorb-structural integration program. The contract required the designing, building and testing of panels for use on re-entry vehicles. These panels would separate the cooled compartment from the high temperatures of re-entry and provide the required structural strength and thermal protection for the vehicle.

This paper presents some useful methods of thermal analysis for use in the design of a thermal protection system, examines the parametric relations involved, and describes test results for comparisons with analytical work.

The basic system considered is shown in Fig. 2 with the system components described as follows: 1) an outside heat shield which cools itself by radiative and/or ablative methods, 2) a layer of insulation to impede the transfer of heat to the inside compartment, 3) a vapor barrier to prevent steam from the Thermosorb from entering the insulation[3], 4) a space between the vapor barrier and Thermosorb to provide an exit for the steam, 5) a layer of Thermosorb to absorb the heat transmitted from the hot exterior surface, 6) a cold wall to provide the basic vehicle structure, 7) supports from the cold wall for the vapor barrier and the exterior heat shields, and 8) a steam venting system.

[3]Systems in which the steam leaves the vehicle through the insulation are possible. However, such systems are not analyzed in this paper.

SYSTEM ANALYSIS

From the viewpoint of heat transfer engineering, the problems associated with system analysis can be separated into three groups. First is the problem of weight as a function of the relative amounts of insulation and heat sink. Second is the problem of weight due to heat shorts. Heat shorts are those structural members necessary to support the vapor barrier and heat shields. Such structure, in terms of heat transfer, provides "shorts" from the hot side to the cold side. Finally, the problem of weight and space required for steam vents is considered. This emphasis upon weight is made with the understanding that reliability and performance requirements will be maintained during the weight reduction process.

Insights into insulation and heat sink weight optimization can be determined by computer methods which simply hold constant a number of parameters and vary the thickness of insulation. When the system weight is plotted against insulation thickness, the minimum weight is found to exist at or near the condition where the weight of the insulation is equal to the weight of the heat sink. Such a plot is shown by Fig. 3. From a rigorous viewpoint, the plot applies only to the particular set of values used for the independent parameters. These independent parameters include such items as heat sink temperature, radiation factor from vapor barrier to heat sink, and insulation conductivity and density. Thus, numerical calculations to determine optimum quantities of insulation and heat sink give particular answers as contrasted to general answers.

Based upon the foregoing considerations, a series of mathematical simplifications were explored in order to understand better the effects of changes in the many independent variables. As working models, three temperature-time profiles were selected to represent suborbital, orbital, and lunar return re-entry conditions. These profiles are shown by solid lines by Fig. 4. Although the straight lines in themselves represent simplifications, the mathematical equations associated with varying hot side temperatures are cumbersome and not readily adaptable to manipulation. In addition, it is known that the insulation and vapor barrier will not contribute much as heat sinks. Therefore, it was decided to transform the selected temperature-time profiles into rectangular pulses and, for the time being, ignore all heat sinks other than the Thermosorb itself. The transformed profiles are shown by dotted lines in Fig. 4. Each profile has an exact transformation, and each rectangular pulse represents a family of profiles. Whether or

not the chosen transformation includes the exact initial profile is somewhat immaterial in establishing parametric relations. After the relations are established and used in panel design, final optimization of panel weight by use of computer methods and the initial profile insure that no accumulation of error will exist.

In working with rectangular pulses and steady-state heat transfer equations, the mathematical difficulties are reduced, and important parametric relations are determined. In setting up equations suitable for determination of minimums by the methods of differential calculus, it is found that the dependent temperature of the vapor barrier involves a fourth order algebraic expression with an eleventh order derivative. It is obvious by simple substitution that the weight of the insulation being equal to the weight of the heat sink does not satisfy the derived equation. Neverthe less, crossplots of solutions obtained by computer methods show minimum weights at or near the equal weights condition for a variety of insulations.

Part of the mathematical difficulty arises from the simple fact that high order algebraic equations are cumbersome. However, much of the problem can be expressed in simple linear relations. For example, the rate of heat transfer from the hot side to the heat sink can be written simply as

$$q_b = K\Delta T/x \qquad [1]$$

where the symbols are listed at the end of the paper and ΔT is the temperature drop across the insulation. Further, the weight of the heat sink is

$$W_w = q_b\theta/h_{fg} \qquad [2]$$

and the weight of the insulation is

$$W_i = \rho x \qquad [3]$$

The weight of the heat sink plus the weight of this insulation is

$$W_s = W_w + W_i \qquad [4]$$

By substitution

$$W_s = (K\Delta T\theta/x h_{fg}) + \rho x \qquad [5]$$

The condition that x be the only variable on the right-hand side of the equation is that there be no thermal resistance

between the insulation and the heat sink. In other words, the insulation takes all the temperature drop. With such conditions imposed, straight differentiation gives

$$dW_s = (K\Delta T\theta/x^2 h_{fg})dx + \rho\, dx \qquad [6]$$

For a minimum, the derivative is equal to zero, or

$$x = (K\Delta T\theta/\rho h_{fg})^{1/2} \qquad [7]$$

The insulation weight is then

$$W_i = \rho x = (K\rho\Delta T\theta/h_{fg})^{1/2} \qquad [8]$$

The heat sink weight becomes

$$W_w = q\theta/h_{fg} = K\Delta T\theta/x h_{fg} \qquad [9]$$

Upon substituting for X

$$W_w = K\Delta T\theta/(K\Delta T\theta/\rho h_{fg})^{1/2} h_{fg} \qquad [10]$$

which is the same expression as was obtained for the weight of the insulation.

It is to be noted that the foregoing derivation did not allow for thermal resistance between the vapor barrier and the heat sink. When such allowance is made, the equations, using q as a parameter, become

$$W_i = (K\rho/q)(T_s - T_{VB}) \qquad [11]$$

$$W_w = q\theta/h_{fg} \qquad [12]$$

$$q = \sigma F_\epsilon (T_{VB}^4 - T_{cw}^4) \qquad [13]$$

Fig. 5 shows a plot of component weight and total weight versus barrier temperature with $K\rho$ as a parameter. Fixed typical values as shown were used for other parameters. The insulation parameter was assigned two values -- 0.5 and 5.0 (Refrasil A-100 has a $K\rho$ of about 0.5). Calculations were made by assigning values to T_{VB}, and then computing the weight figures. The process reveals important cues as to what determines minimum weight.

Notice that only one curve exists for the heat sink weight W_W, while two curves each are shown for the system weight W_S and the insulation weight W_I. For the 1-hr. time period considered, the required weight of the heat sink is simply a fourth power function of T_{VB}. In calculating the weight of the insulation, the term T_{VB} appears as a first power in the numerator as a fourth power in the denominator. This means that the weight of the insulation is a modified inverse fourth power function of T_{VB}. The system weight is simply the sum of the two component weights. The insulation weight continuously decreases with increasing T_{VB}, and the heat sink weight continuously increases with increasing T_{VB}. The minimum system weight occurs when the slopes of the two functions are equal. That is, beginning with low values of T_{VB}, and going upward, a point is reached at which the next ΔT_{VB} costs as much in heat sink weight as is saved in insulation weight. Notice that the minimum system weight occurs at or near the point where the two component weights are equal, and, for the more realistic value of $K\rho = 0.5$, the bottom of the system weight curve is reasonably flat.

In the first simplified system in which there is no vapor barrier or radiative resistance, it is determined that the minimum-weight-system insulation requirement may be determined by equation 8. That is, the required weight of the insulation would increase with the square root of the $K\rho$ quantity for the insulation. From Fig. 5, it is noted that, for a $K\rho = 0.5$, the system minimum weight is 2 lb/ft^2, and that, for a $K\rho = 0.5$, the system minimum weight is 5.9 lb/ft^2. The ratio of $K\rho$'s is 10, and the square root of 10 is 3.16. If the square root ratio were true, then the weight of the heavy system extrapolated from the lighter system would be 2 times 3.16 = 6.32 lb/ft^2 as compared to the calculated and plotted value of 5.9 lb/ft^2. The primary difference between the two numbers is due to the radiative resistance which reduces requirements for both weight components. Nonetheless, the numbers serve to establish a criterion for insulation and show that it is better to compare the ratio of the square root of the $K\rho$ values than it is to make comparisons on the basis of K or ρ or upon the first power of $K\rho$.

Another cue derived from Fig. 5 is that, regardless of the type of insulation used, the minimum weight system will have approximately equal weights of insulation and heat sink. This fact makes possible a technique for rapid hand calculations for use in exploring the effect of other independent variables. For example, the effects upon optimum system weight of varying the radiation emissivity factor between the vapor barrier and the

Thermosorb are quite easily determined by only a few iterations. By assigning fixed values to the other independent variables, and using several values for the emissivity factor, it is possible to calculate the approximate optimum system weight for each emissivity value. This is done by selecting a value for vapor barrier temperature, computing the heat radiated to the heat sink, using the resulting heat sink weight as the insulation weight, and then computing the vapor barrier temperature in terms of the temperature drop from the heat shield to the vapor barrier. Iteration is used until the selected and computed vapor barrier temperatures agree. The weights used in the last iteration represent the optimum system weight for that value of the emissivity factor. When such computations are completed, the system weight is then plotted as a function of the emissivity factor, and the desired relation is obtained. Thus the addition of one equation, $W_w = W_{\dot{c}}$, represents a tool far more powerful than is indicated by the simplicity of the equation.

Although variations exist in the use of the equal weights equation, all such methods are based upon the following: 1) the weight of insulation is equal to the weight of the heat sink, 2) the heat transferred through the insulation is equal to the heat absorbed by the heat sink, and 3) the temperature of the vapor barrier is the same when approached from either side.

The use of cross plots such as Figs. 3 and 5 and the simplified relation shown by

$$W_s = 2\left(K_\rho \Delta T \theta / h_{fg}\right)^{1/2} \qquad [14]$$

can be used as the basis of extended parametric studies. For example, the heat of vaporization of water increases with decreasing boiling temperatures. Reference to the foregoing equation shows that the approximate effect upon system weight due to decreasing cold wall temperatures is to reduce the system weight by an amount inversely proportional to the square root of the ratio of the heats of evaporization. By treating superheat as an increase in h_{fg}, the same argument and approximations may be used. Since ΔT is the difference between the hot and cold sides, variations in these parameters are further traced by the same equation. Finally, note that the system weight increases with the square root of the time duration of the mission. This means, for example, that the longer the mission, the lower the temperature of the vapor barrier, and vice versa. Equation 7 provides a first approximation to the insulation thickness when considering how thick the panel

should be while equation 14 provides in algebraic form a first approximation to parametric relations. Crossplots such as Fig. 3 assist in understanding the relations. Iterative calculations using equations 1 and 13 and the assumption that $W_c = W_w$ provides readily available numerical approximations. Finally, computer methods refine the answers to provide true optimum design. The composite effect is that the parametric relations are defined, understood, and reduced to design practice.

The trajectory that will be used on a re-entry mission depends upon many factors beyond the scope of this paper. One way to compare the effect that varying trajectories have upon the weight of the compartment cooling system is to plot the system weight versus the total mission heat flux to the vehicle outer skin. Fig. 6 shows such a plot for varying heat fluxes due to different types of re-entry. A given mission probably would not have as much spread, but the trend would be approximately the same.

Fig. 6 also shows the effect of various values of K_ρ upon system weight. As expected, the greater the heat flux, the greater the effect that K_ρ has on the system.

Fig. 7 shows the effect of the emissivity factor between the vapor barrier and the Thermosorb as well as the effect of varying cold wall temperatures. The low emissivity factor appears attractive until the effects of Fig. 8 are considered. The lower vapor barrier temperatures associated with the higher emissivity factor of 0.5 would be much more desirable than an emissivity of 0.1 from this point of view.

By using the methods developed, the effects of any of the heat transfer-weight relations may be plotted, and those shown illustrate this idea.

Heat transfer from the hot side to the cold side by conduction along the supporting structure is known as "heat short" effects. At first, it would appear that the heat short effects could be simply calculated by use of variations of the conduction equation. However, the interplay of heat transfer between the supports and the insulation, the effects of contact resistances, and the multitude of conduction paths lead to complex equivalent analog circuits.

The design of the supporting structure is best begun only after the general thickness of insulation and heat sink material has been established. For initial working purposes,

the thickness allowed for the heat sink material should include enough vent area to prevent excessive steam velocities and should allow for the addition of heat sink to absorb the heat transferred by the structure. In general, this means that the allowed thickness for the heat sink and vent area will be of the order of 0.2 to 0.3 in. compared to a much larger thickness for the insulation. Thus the length of the supports can be estimated early in the preliminary design.

The area associated with each support will depend to a large extent upon the design of the heat shield and the aerodynamic loading. In arriving at initial designs, one of the things that must be considered is the manner of distributing the heat that is transferred by the supports. To do otherwise would be to invite hot spots on the cold wall.

As additional aids in assessing the final conductivity of the support configuration, it is convenient to develop resistance-capacitance transforms for circular washers, truncated prisms, and other geometric forms amenable to the methods of ordinary calculus. Sections of the supports then may be approximated and assigned values of resistance and capacitance for use in both hand and computer calculations. Additional heat sink material is needed to absorb the heat transferred by heat shorts. This additional weight should be added to the weight of heat shorting structure in comparing proposed structural designs.

A number of useful concepts are available for use in steam system design. The ideal gas laws apply to most conditions, but it is much more convenient to use thermodynamic charts such as those of Ellenwood and Mackey.[4] These charts plot enthalpy versus volume with parameters of pressure, temperature, and entropy. The end points of processes such as throttling and isentropic expansions can be read directly from the charts, and the saving in time becomes significant.

For other purposes in which there is no serious question about the degree of superheat so that the ideal gas laws apply, a useful plot is that shown by Fig. 9. The plot shows the pressure ratio vs fL/D for varying inlet Mach numbers. fL/D is a parametric measure of fluid flow carrying capability of, for instance, a length of duct, and the pressure ratio is the ratio

[4]Ellenwood, F.O. and Mackey, C.O., Thermodynamic Charts (John Wiley and Sons, New York, 1949), 2nd ed.

of outlet to inlet pressure. The limiting condition shows the pressure ratio that is possible for given inlet Mach number. The plot is based upon adiabatic conditions and is usually found in textbooks on fluid flow. Fig. 9 also illustrates the importance of inlet Mach number on steam vent design. Notice that the median between pressure ratio and allowable fL/D occurs at or about an inlet Mach number of 0.1 instead of the intuitive 0.5 which is halfway between no flow and choked flow.

The inlet Mach number is limited by another consideration. Velocities in excess of 0.1 acoustical velocity across the heat sink might cause excessive erosion of the heat sink material. As such, the height of the vapor barrier above the heat sink should be sufficient to keep the Mach number down to the range of 0.1 for both possible scrubbing and pressure drop reasons.

The steam vent system might contain a pressure relief valve to keep the venting pressure from falling below a given value even though such a valve is by no means a mandatory requirement. If a valve is used, a question arises as to whether or not the steam expansion will cause freezing. In making this check, it is important to remember that the expansion process is more throttling than it is isentropic. Reference to thermodynamic charts show the temperature drop associated with the constant enthalpy of throttling is not near as great as in the case of isentropic expansion. Therefore, borderline freezing conditions uncovered by isentropic processes may well turn out to be of no importance.

Fig. 10 shows the required distance between the heat sink and vapor barrier when a square foot of area is vented all along one side. Notice the rapid increase with decreasing boiling temperatures. Fig. 11 shows the required valve flow area in square inches per square foot of panel for various heat sink temperatures. The numbers apply only to a specific vent configuration but serve to illustrate another important point. If a heat sink temperature of, say, 80°F is selected for a given valve flow area and given heat rate input, the plot shows how the heat sink temperature will rise with increasing heat inputs. Conversely, the plot may be used to show the effects of a failed open valve. If the valve fails in the open position, the temperature drops, but the increasing steam volume is so great in the region of 50°F that even the failed open valve chokes. In fact, suitable systems can be designed which use a fixed opening instead of a valve, and thus eliminate the only moving part in the system. After a vent system is designed from the foregoing considerations, the weight is readily determined. Thus, several geometric arrangements can be considered.

TEST RESULTS

Two vehicle wall panels were fabricated for tests. These panels were designed to withstand 1800°F on the hot side. The heat sink material was used to maintain cold wall temperatures. Tests were conducted using radiant heating lamps, thermocouples, and a special balance to measure weight loss. Thus the rate of heat transfer could be calculated from the measured rate of weight loss and the heat of vaporization of the heat sink material.

One of the first analytical assumptions tested was that the heat transfer from the vapor barrier to the heat sink would be by radiation with only negligible effects due to conduction and convection. Fig. 12 shows a plot of heat flux versus vapor barrier temperature. The close agreement of the data with a mathematical fourth order curve shows the validity of the assumption.

Fig. 13 shows the $K\varrho$ under actual use as compared to values furnished by the insulation manufacturers. Considering possible experimental errors, the difference is small. Fig. 14 gives a measure of the predictability of vapor barrier temperature, and the test results are encouraging.

Fig. 15 shows the effects of heat shorts for a truss core type panel and a beam type panel construction. In general, the heat short effects are at least as great as conduction calculations would indicate even when joint resistances are assumed to be zero.

Fig. 16 shows some interesting results due to small uninsulated area. At first, these results seem unreasonable, but a comparison of the increase with the radiation potential of the hot heat shields shows that the results could be expected. The curve shown is for a heat shield temperature of 1800°F.

Fig. 17 shows the change in cold wall temperature as a function of steam chamber vent pressure. The cold wall is warmer than saturation temperatures primarily because of heat short effects.

Finally, Fig. 18 shows a complete panel operating with a hot side temperature of 1740°F -- a temperature near the upper limit of the uncoated steel heat shields used for the particular series of tests. The insulation was nominal 1/2 in. thick, 6 lb/cu ft micro-quartz. The steam vent pressure was 1.6 psia. The cold wall temperature was 135°F -- only 17°F above the

saturation temperature of water at the same pressure.

The test does not represent a particular temperature-time profile. Instead, the insulation thickness was arranged to give a vapor barrier temperature above 700°F, i.e., near the upper value expected for any re-entry condition.

The stable cold wall temperature that follows the initial transient is evidence of the cooling effect of the heat sink, and thus the proof-of-principle of the system concept is demonstrated.

CONCLUSIONS

The following is a list of conclusions based upon the analysis and test results: 1) the simplified methods of analysis described herein are adequate for preliminary design considerations, 2) the use of manufacturer's insulation material properties will provide adequate correlation between predicted and actual insulation performance, 3) additional heat sink weights required to compensate for structural heat shorts may best be established by testing the specific design concept, 4) care should be taken to insure proper installation of insulation in a vehicle and packaging provided to insure that the insulation will maintain its position during flight, and 5) finally, the ability of the thermal protection concept described herein to provide adequate protection to crew or equipment has been demonstrated.

NOMENCLATURE

q_D = heat transfer rate, Btu/hr-ft^2

K = conductivity (Btu/hr) (ft/ft^2 ^oR)

A = area, ft^2

ΔT = temperature difference, ^oR

χ = thickness, ft

W_w = weight of heat sink, lb/ft^2

θ = time, hr

h_{fg} = latent heat of vaporization, Btu/lb

W_i = weight of insulation, lb/ft^2

W_s = system weight (W_w + W_i)

ρ = specific weight, lbs/ft^3

F_ϵ = radiative view factor

T_s = hot side temperature, ^oR

T_{vb} = vapor barrier temperature, ^oR

T_{cw} = cold wall temperature, ^oR

$\frac{fL}{D}$ = fluid flow friction factor (length)/diameter

N_m = Mach number

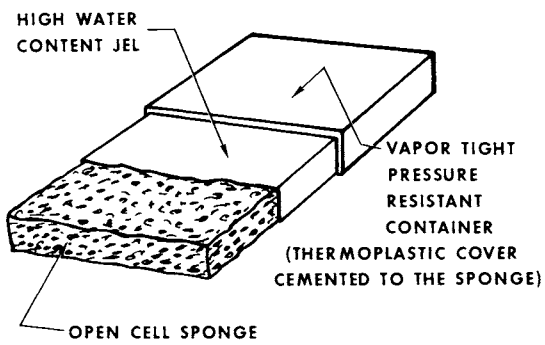

Fig. 1 Thermosorb heat sink schematic

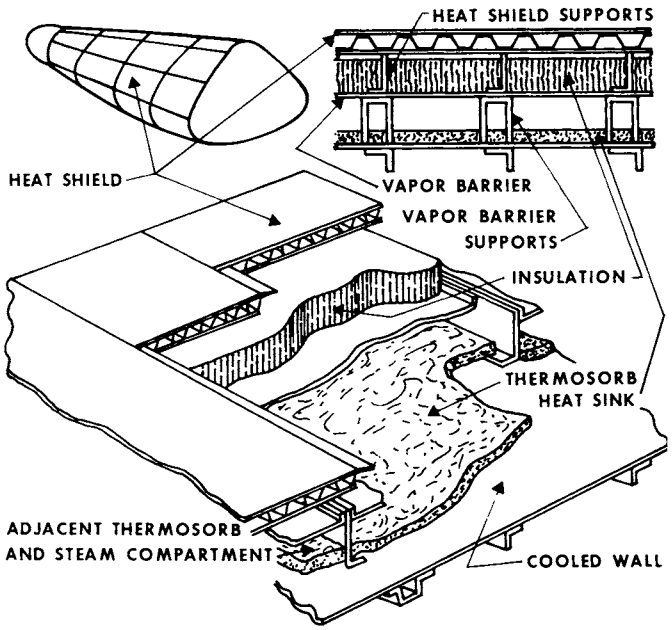

Fig. 2 Thermosorb thermal protection system schematic

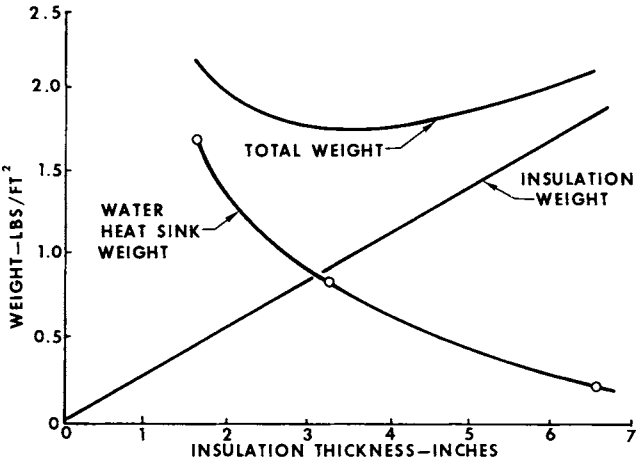

Fig. 3 Thermal protection system weight optimization

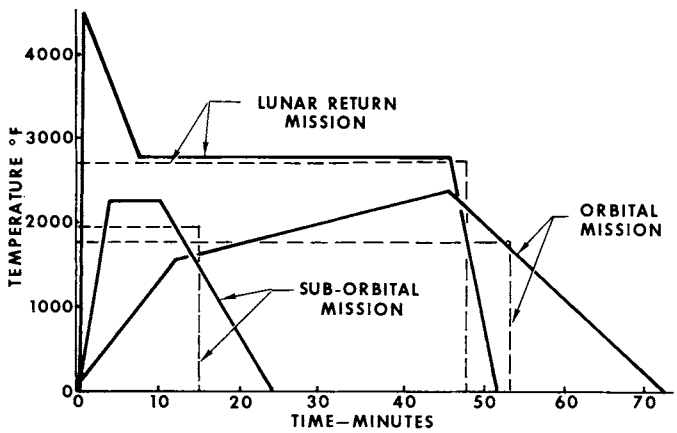

Fig. 4 Transient and simplified temperature profiles for various re-entry missions

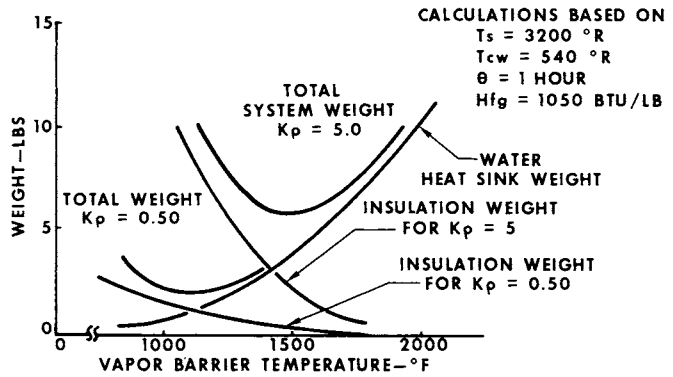

Fig. 5 Optimum system weight variation with insulation conductivity and density

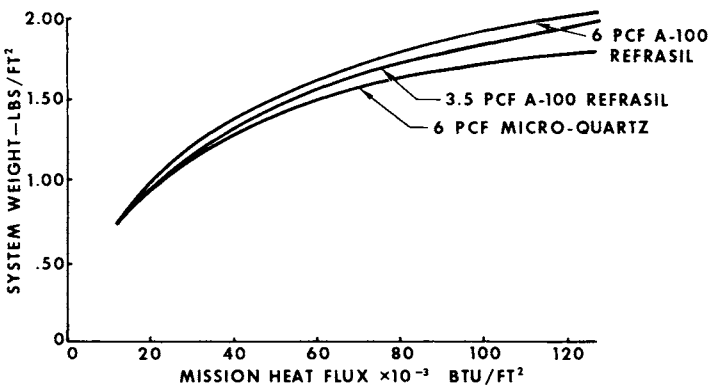

Fig. 6 Effect of insulation type on thermal protection system weight

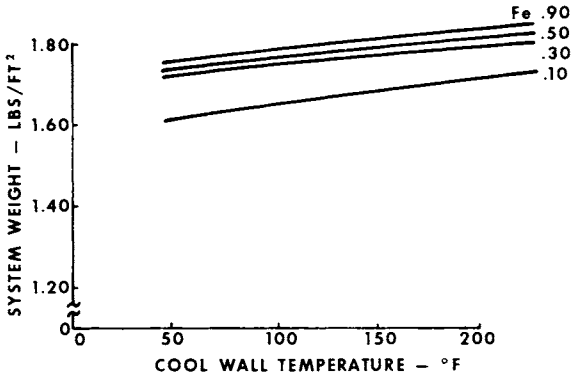

Fig. 7 Variation in optimum system weight with radiative view factor. Lunar mission profile using 6 lb/ft^3 micro-quartz insulation

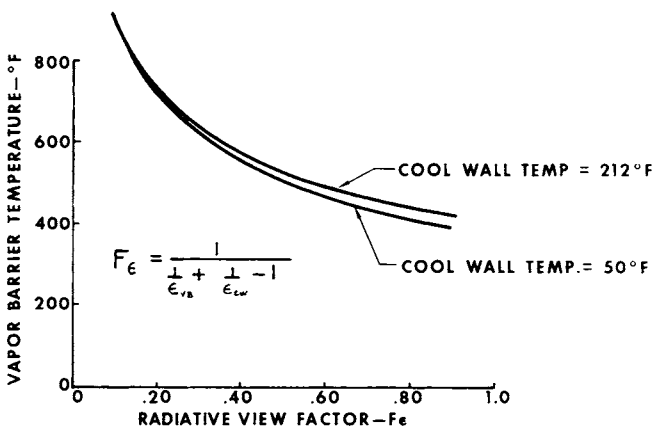

Fig. 8 Effect of radiative view factor on vapor barrier temperature

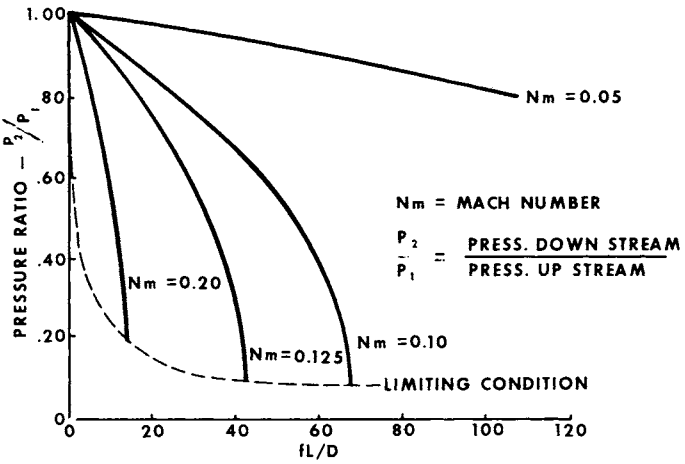

Fig. 9 Variation in pressure ratio with mach number and fL/D

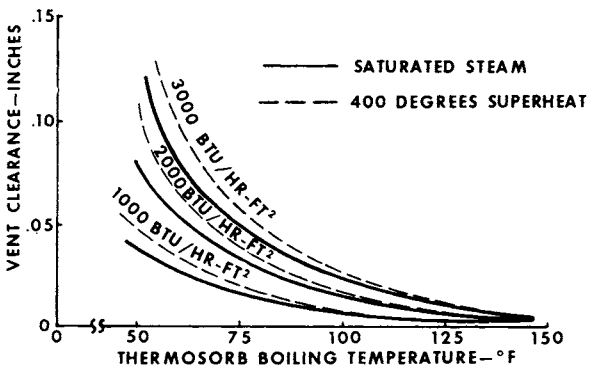

Fig. 10 Vent clearance requirements

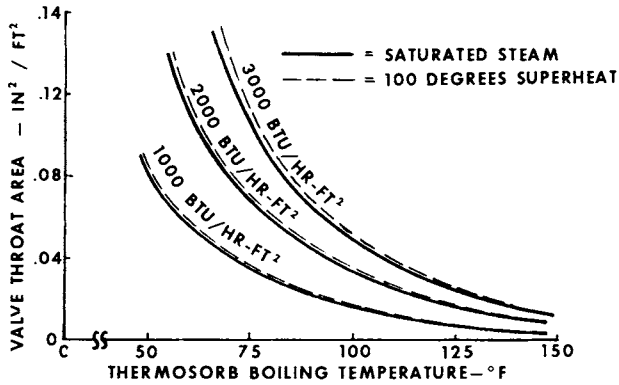

Fig. 11 Valve throat area requirements

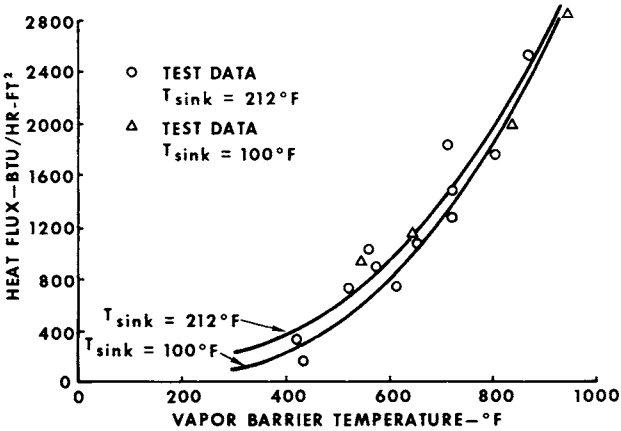

Fig. 12 Heat absorbed by thermosorb. Solid lines represent calculated values

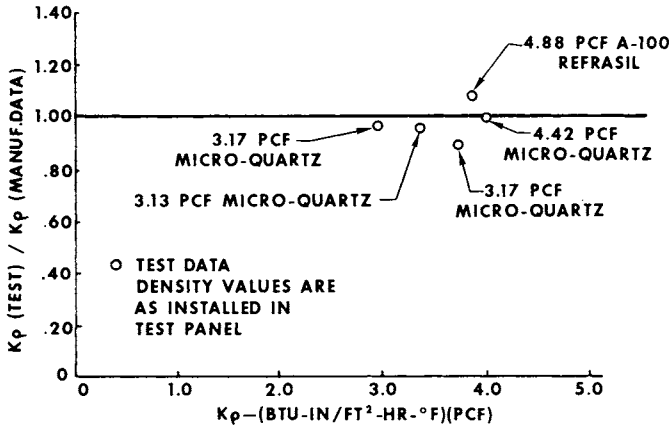

Fig. 13 Correlation of test and published values of insulation

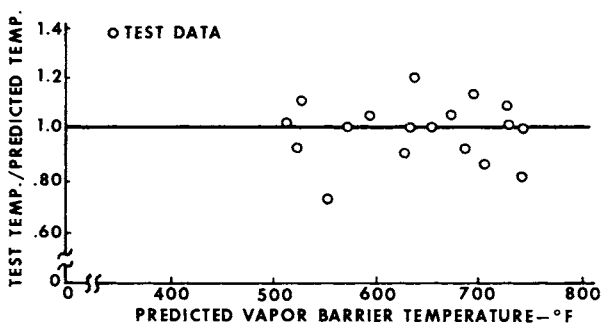

Fig. 14 Correlation of test and calculated vapor barrier temperatures

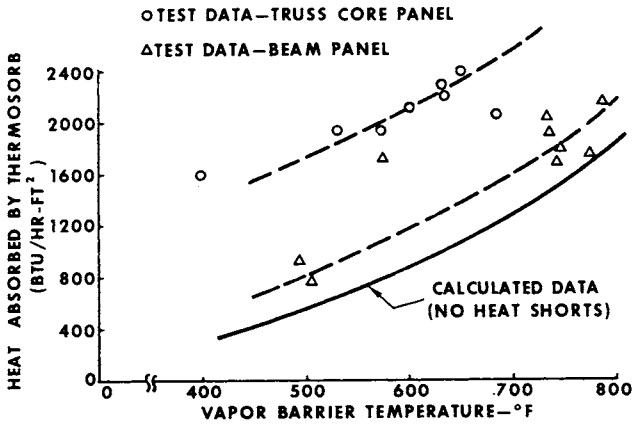

Fig. 15 Heat short penalty due to structural supports

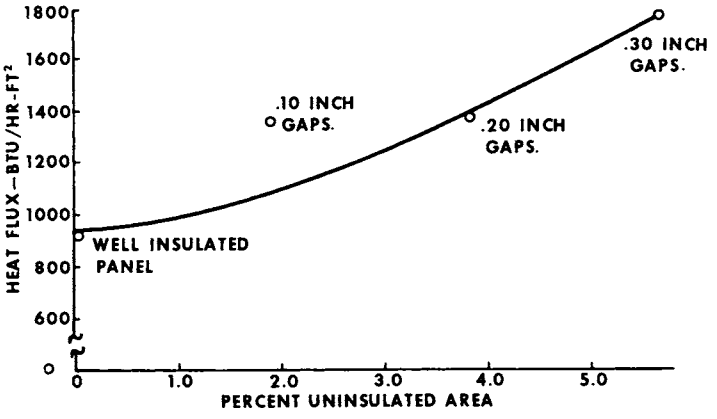

Fig. 16 Increase in heat absorbed by the thermosorb due to separations in the insulation

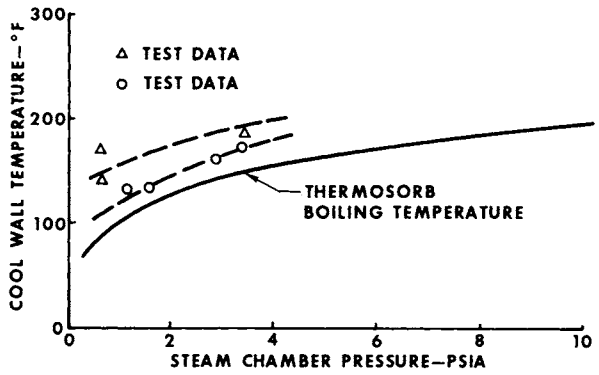

Fig. 17 Cooled structure temperature variation with vent chamber pressure

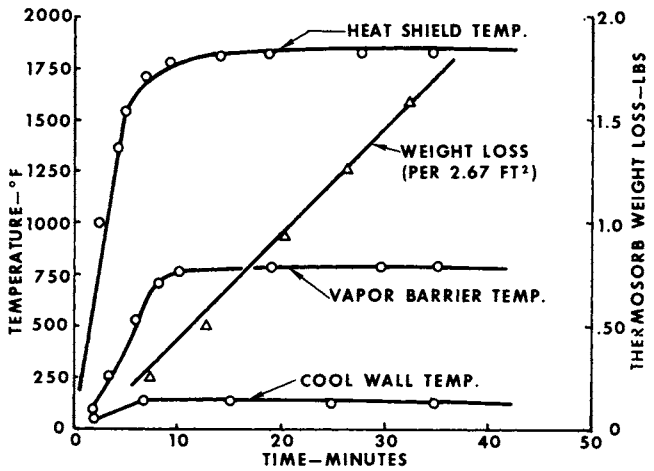

Fig. 18 Thermal protection system performance under test conditions